Hybrid control test of connections for buckling restrained braces in RC continuously braced frames

Z. Qu, Y. Maida, M. Nonoyama, S. Kishiki, H. Sakata & A. Wada
Structural Engineering Research Center, Tokyo Institute of Technology, Midori, Yokohama, Japan

Keywords: hybrid control test, connection, buckling restrained brace (BRB), reinforced concrete, continuously braced frame (CBF)

ABSTRACT: A continuously braced frame system is proposed and a hybrid-control test, in which BRBs are simulated by force controlled actuators, is carried out to assess the performance of the proposed connections for BRBs. Results show that the deformation in the connection is very small and would not impair much the effectiveness of the BRBs to dissipate energy. The influence of the BRB gusset plate to the deformation and cracking pattern of the reinforced concrete components is also insignificant.

1 INTRODUCTION

Extensive experimental studies have been carried out ever since the advent of buckling restrained braces (BRBs). These experiments often include axial loading tests of individual BRBs (e.g. Watanabe 1988, Black 2001) or subassemblage tests of steel frames with BRBs (e.g. Hori, 1991; Kamiya, 1997). Pesuodo dynamic test and shaking table test were also carried out on complete steel buckling-restrained braced frames (e.g. Tsai, 2008). Most of these experiments focused mainly on the hysteretic performance of the BRBs themselves while some attention was also given to the BRB connections.

In contrast to the extensive research and wide applications of BRB in steel frames, its application in reinforced concrete structures are few and primarily in the field of retrofit of existing buildings. Subassemblage tests were carried out in Japan on RC frames retrofitted with BRBs (e.g. Ishii, 2004; Satsukawa, 2005). Ogawa et al (2004) reported on one of the few, if not the only, attempts to apply BRB in newly-built RC structures, in which the gusset plate of BRB extends into the concrete components and are anchored inside by wide flange steel beams or steel rebars. Subassembly test was carried out and the result proved that the impairment of the connection deformation to the effectiveness of BRB is insignificant.

Taking advantages of the stable hysteresis of BRB, the use of real BRBs can be avoided in tests focusing only on the behavior of BRB connections, where the force transmitted to the connection and thus to the rest of the structure can be simulated by a force-controlled actuator. In such a manner, the test setups can be greatly simplified and the cost of the test can be reduced. As a result, more attention could be paid on the BRB connections themselves.

2 CONTINUOUSLY BRACED FRAMES

As an effort to promote the application of BRB in newly built RC structures, a continuously braced frame system (CBF, Figure 1a) is proposed. In a CBF, braces in neighboring stories in the same span share the same gusset plate so that all the braces in this span run continuously along the

height of the structure. The gusset plate is attached to the RC joint surface rather than to the column ends or beam ends and the impairment of the slenderness of columns can be minimized.

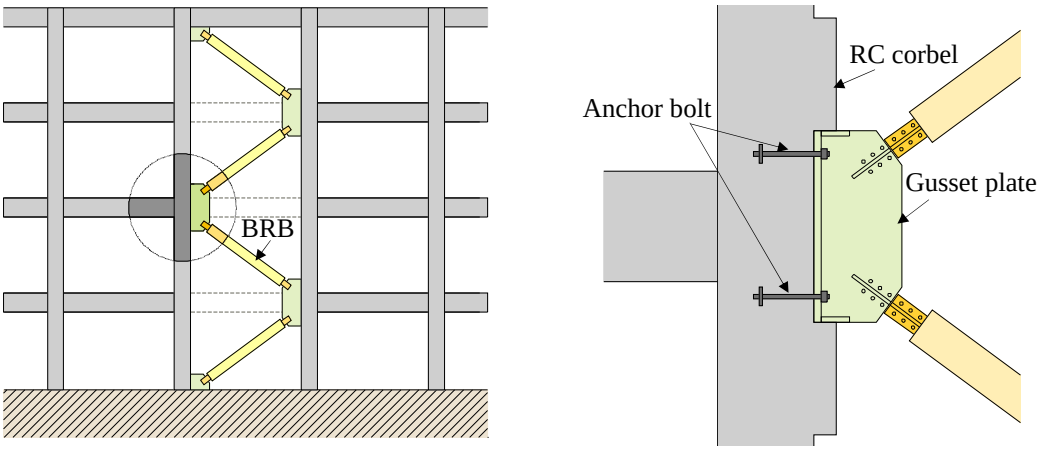

Figure 1. RC continuously braced frame: a) BRB arrangement b) BRB connection

The gusset plate is fastened to the joint surface by anchor bolts to resist possible horizontal tensile forces. As the vertical components of forces transmitted to the gusset plate would be as large as the sum of the BRB yield strength, a pair of reinforced concrete corbels on both lower and upper side of the gusset plate is used to provide not only adequate shear strength to encase the gusset plate, but also large stiffness to minimize the vertical displacement of the gusset plate (Figure 1b)

3 EXPERIMENTAL PROGRAM

The purpose of the experiment is to verify the performance of the proposed BRB connections in CBF. The primary concerns are: (1) whether unintended damages to the RC frame components would be imposed; (2) whether the deformation of the connections is small enough not to affect the effectiveness of BRBs. Hybrid controlled quasi-static test is carried out for 1/2 scaled subassemblies of an archetype continuously brace frame. Details of the specimens and the loading systems are described below.

3.1 *Test specimens*

The 1/2 scale subassembly is taken from a CBF with 5.6m span and 4.0m story height. In the test, the specimen is pinned at the inflection points of the column and the beam (assuming at the center of the column and the beam). The column is pre-compressed by 4 post-tensioned steel rods to bear a 500kN initial axial compressive force, which is about 6.25% of the nominal compressive strength of the concrete (50MPa) multiplied by the gross cross section area of the column (400mm× 400mm).

Concrete corbels protruding from the column surface are cast together with the column. Between the corbels, the steel gusset plate is inserted and fastened to the anchor bolts embedded in the concrete joint. A thin Teflon plate is place between the gusset plate and the concrete joint surface to reduce the friction. The bolts are then pre-tensioned to increase the initial stiffness of the connection. High strength grout (123MPa) is injected to fill the 10mm gap between the gusset plate and the corbels.

A total of 4 specimens are tested. Detail of the standard specimen (i.e. Specimen No.1) is depicted in Figure 2. Three parameters are investigated, namely the beam size, the amount of lateral reinforcement in the corbel and the pre-tension force in the anchor bolts. Major parameters are listed in Table 1 and the items that are different from Specimen No.1 are marked in bold.

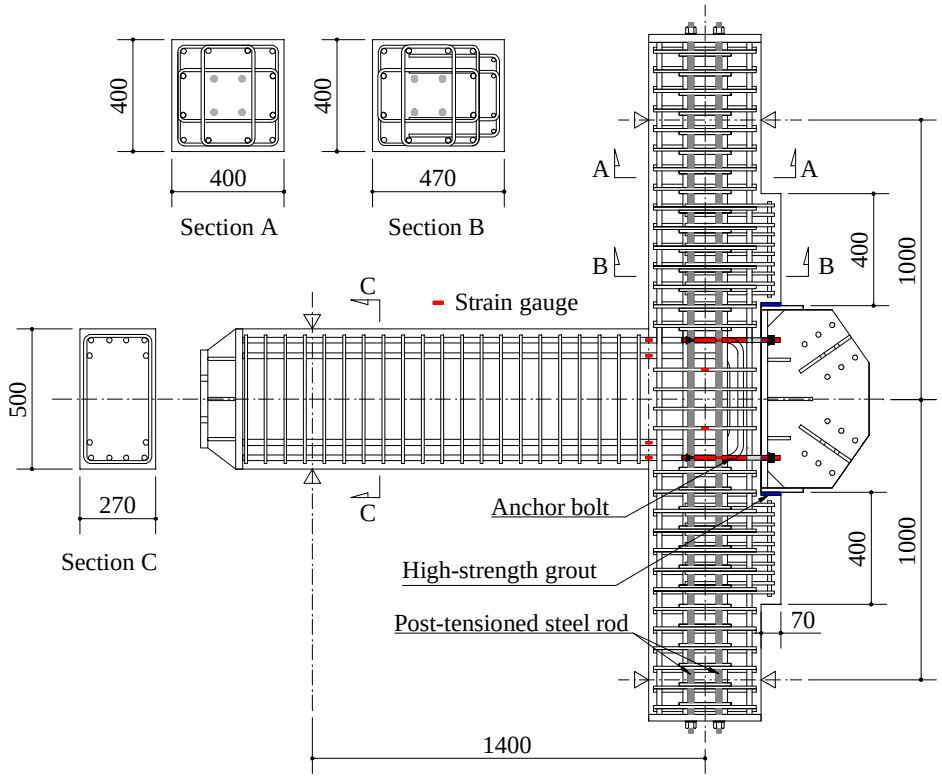

Figure 2. Dimensions and reinforcement of Specimen No.1 (Standard)

Table 1. Specimen parameters

	No.1 Standard	No.2 Small beam	No.3 Weak corbel	No.4 Enhanced anchor
Beam dim. (mm)	270×500	**350×300**	270×500	270×500
Main rebars in beam	6-D19	**4-D19**	6-D19	6-D19
Stirrups in corbel	D10@70 - 4 legs	D10@70 - 4 legs	**D10@70 - 2 legs**	D10@70 - 4 legs
Pre-tension in bolt	30kN/piece	30kN/piece	30kN/piece	**60kN/piece**
Column dim. (mm)	400×400			
Column main rebars	12-D19			
Column lateral rebars	D10@70 - 4 legs			
Beam lateral rebars	D10@70 - 2 legs			

The average compressive strength of the concrete is 58.2MPa and that of the high strength grout is 123MPa. The average yield strength of D19 rebar is 519MPa for the column and 438MPa for the beam. The average yield strength of the lateral rebars is 346MPa.

3.2 *Experimental setup*

The use of real BRBs is avoided in the test. Instead, two 500kN hydraulic actuators are connected to the gusset plate and are used to simulate the axial forces of the BRBs belonging to the lower and upper stories. Another 200kN actuator is connected to the leftmost end of the beam to balance the possible horizontal resultant of the BRB forces. These three actuators are force controlled to simulate the loading, yielding and unloading of the BRBs. The specimen is driven to story drift targets by a displacement controlled 1000kN actuator at the top end of the column. A schematic diagram of the experimental setup is given in Figure 3.

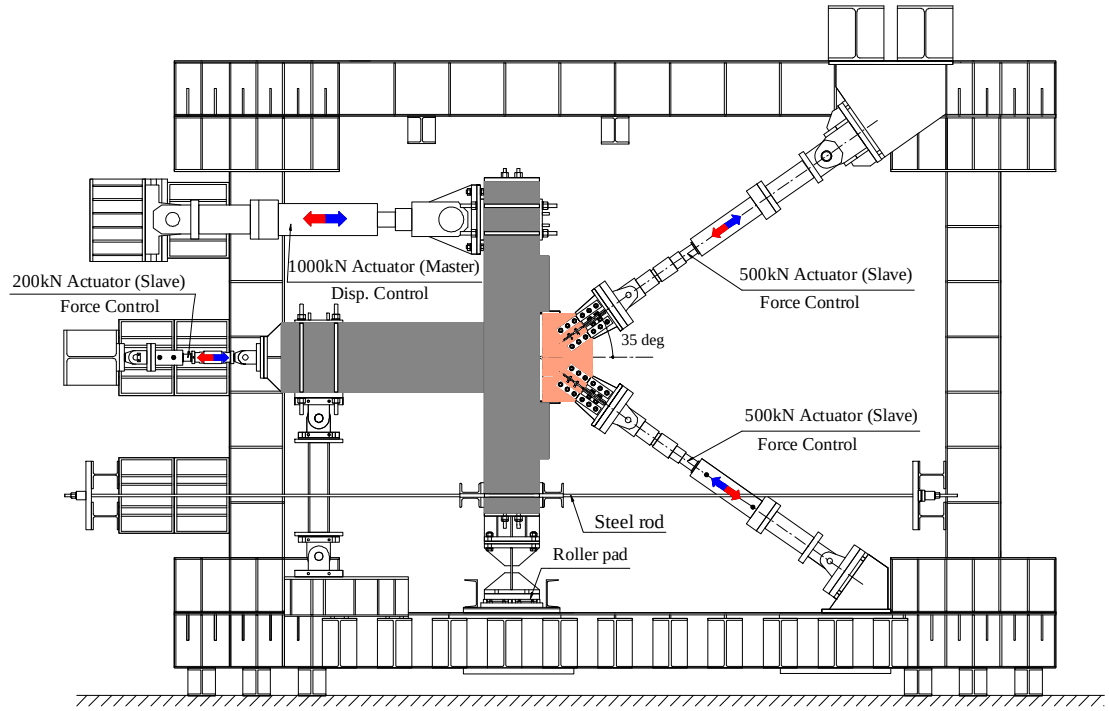

Figure 3. Side view of the experimental setup

3.3 *Loading control*

Denote the displacement imposed by the 1000kN jack at the top end of the column as δ. The story drift ratio θ of the specimen is then δ divided by the story height, i.e. 2000mm for the 1/2 scaled specimen.

In every loading increment, the specimen is first loaded to the target story drift ratio of the current increment by the 1000kN master actuator. The 3 slave actuators (i.e. the two 500kN actuators representing the BRBs and the 200kN actuator at the beam end) are then adapted to their target forces which are calculated from the current story drift according to the following method.

When the specimen is deformed, the corresponding change in the work point-to-work point brace length (denoted as δ_D) is calculated following the linear geometry from the story drift δ and the corresponding story drift ratio θ (Equation 1). Figure 4 illustrates the derivation of this deformation, in which Point A and B are the original work points of the BRBs and A' and B' are the work points after the specimen is deformed.

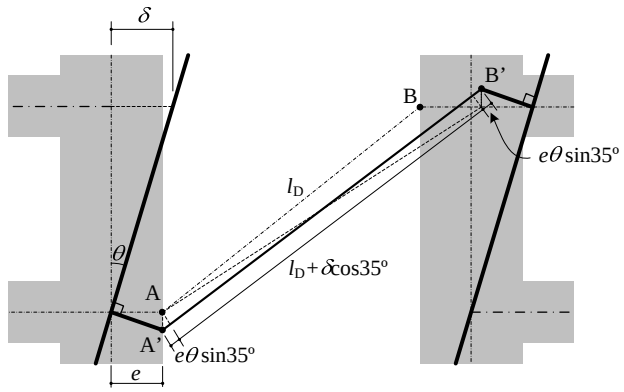

Figure 4. Change in the work point-to-work point brace length

$$\delta_D = \delta \cos 35° + 2e\theta \sin 35° \quad (1)$$

where e is eccentricity of the BRB work point with respect to the column and beam centerlines.

Instead of directly measuring the story drift δ, the beam end deflection relative to the rigid body motion of the specimen is monitored (denoted as δ_B). Story drift δ can then be readily obtained as $H\delta_B/L$, where H=2.0m is the story height and L=1.4m is the half span length. The rigid body motion of the specimen is represented by an aluminum gauge holder, which is attached to the column by a bolt pin on the lower end and a vertical loose-hole on the upper end of the column (Figure 5). In such a manner, the gauge holder moves along with the column without being stretched or bent.

With the gauge holder, the overall deformation of the BRB connection relative to the rigid body motion of the specimen can be measured. Two displacement transducers are mounted diagonally over the gusset plate, connecting the ends of the BRB splice connections and the normal projection of the BRB work point on the gauge holder (Figure 5). The thus obtained displacement is denoted as δ_L since it represents the loss of deformation in the connection, which is a complicated combination of the deformation of the gusset plate, the deformation of the concrete joint, and the relative displacement between the gusset plate and concrete joint.

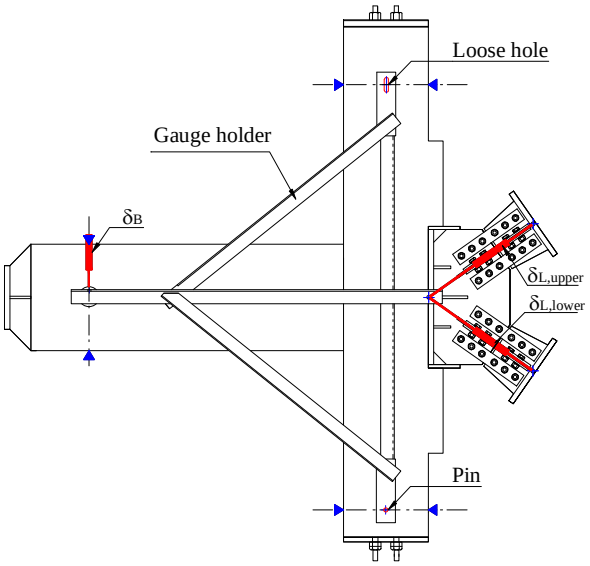

Figure 5. The gauge holder and locations of displacement transducers

The effective axial deformation of the BRB is calculated by subtracting δ_L from δ_D (Equation 2), from which the target forces of the 500kN slave actuators representing the BRBs can in turn be obtained by Equation 3. The target force of the 200kN slave jack acting on the end of the beam is simply equal to the horizontal resultant of the forces of the two 500kN diagonal actuators.

$$\delta_{BRB} = \delta_D - 2\delta_L \quad (2)$$

$$F_{BRB} = \min\left(\frac{EA\delta_{BRB}}{l_D},\quad F_y\right) \text{ during loading} \quad (3a)$$

$$F_{BRB} = F_y - \frac{EA(\delta_U - \delta_{BRB})}{l_D} \text{ during unloading} \quad (3b)$$

where E and A is the Young's modulus and cross section area of the steel core of the BRB, respectively; l_D is the work point-to-work point brace length; δ_U is the BRB deformation at the beginning of unloading; F_y is the BRB yield strength.

For all the specimens except No.4, the yield strength of the lower BRB is set to be 350kN and the upper is 300kN. For No.4, the yield strength of the lower BRB is 300kN and the upper is 100kN so that larger normal force will be imposed on the gusset plate.

The specimens are subjected to a loading program consisting of a series of increasing displacement amplitude cycles. The prescribed amplitudes and the corresponding numbers of cycles are listed in Table 4.

Table 4. Number of loading cycles

	Story drift amplitude					
	1/500	1/200	1/133	1/100	1/50	1/33
No.1 Standard	2	2	-	2	1	1
No.2 Small beam	2	2	2	2	1	1
No.3 Weak corbel	2	2	-	2	1	1
No.4 Enhanced anchor	2	2	2	2	1	1

4 EXPERIMENTAL RESULTS

4.1 *Reinforced concrete frame subassemblies*

Figure 6 plots the hysteretic curve of the story drift ratio θ and column shear force of Specimen No.3. The increments when the BRBs first yield, when the main reinforcement in the beam first yields, and when the hoops in the beam-column joint first yield are marked on the curves and their corresponding story drift ratios are given in Table 5. The locations of the strain gauges are depicted in Figure 2.

For all the four specimens, BRBs start to yield at an early stage with very small story drift ratios, under which the RC subassemblies remain almost intact. Beams with 500mm depth yield at about 1/200~1/160 story drift ratios while the yield story drift ratio of the 300mm beam is slightly larger, about 1/140. What follows is the yielding of the hoops in the beam-to-column joint with the exception of Specimen No.2, the beam of which is of much smaller depth than the others. The main reinforcement of all the columns remains elastic throughout the test.

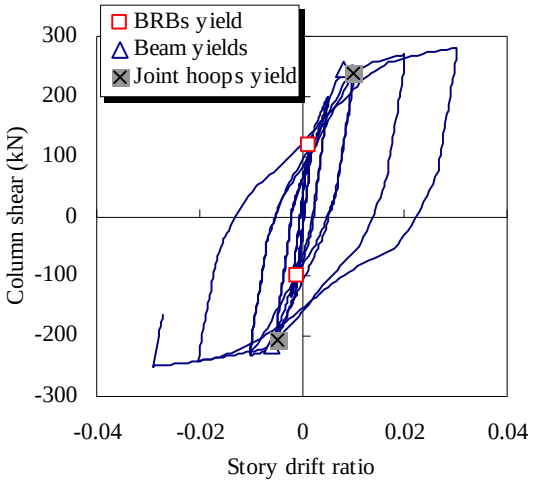

Figure 6. Story drift ratio-column shear relation of Specimen No.3-Weak corbel

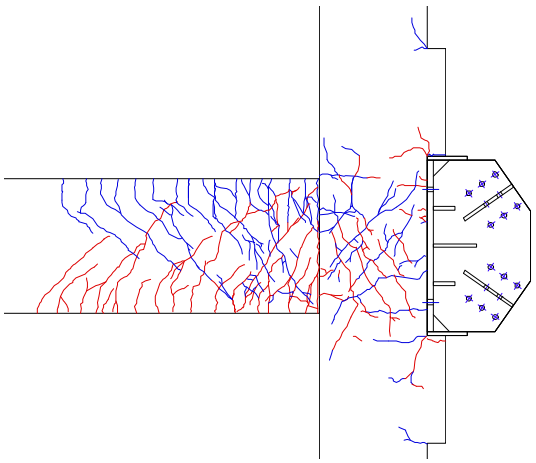

Figure 7. Cracking pattern of Specimen No.3-Weak corbel at 1/33 story drift ratio

Table 5. Story drift ratios at representative increments

	No.1 Standard		No.2 Small beam		No.3 Weak corbel		No.4 Enhanced anchor	
BRBs yield	1/714	(1/972)	1/654	(1/972)	1/673	(1/972)	1/864	(1/1944)
Beam rebars yield	1/163	(1/243)	1/144	(1/148)	1/159	(1/205)	1/164	(1/201)
Joint hoops yield	1/71	(1/130)	-		1/100	(1/205)	1/60	(1/40)

Note: The numbers in brackets indicate the story drift ratios in the opposite direction

Figure 7 plots the cracks of the Specimen No.3 at 3% story drift. Well-distributed shear-flexural cracks are observed in 500mm beams while the cracks in the 300mm beam are primarily flexural ones.

Cracks on the columns are mainly confined within the joint panel zones, which are diagonal shear cracks that are quite typical for reinforced concrete moment resisting frames. It can be confirmed from the test result that the proposed connection does not affect much the behavior of the RC components and impose no considerable additional damages to either the columns or the beams. This advantage adds to the confidence in applying BRBs in reinforced concrete frames.

Cracks initiated from the concaved edges of the concrete corbels are also observed, as can be seen in Figure 7. Some of these cracks are simply the result of the column bending, while others may suggest shear cracking of the concrete corbels. However, the strain readings of the stirrups in the concrete corbels suggest no yielding of these rebars and thus that the damage to the concrete corbels of all the specimens is minor, although the stirrup strain in the corbels of Specimen No.3 is considerably larger than that in the other specimens.

4.2 *Deformation loss*

Figure 8 plots the deformation versus the axial force of the lower BRB in Specimen No.3. As can be seen from Equation 3, BRB axial force is simulated by elastic-perfectly plastic hysteresis. The BRB hystereses in terms of the work point-to-work point deformation (WP-WP) and the effective deformation of the BRB are compared in Figure 8(a) and the deformation of the BRB connection (referred to as δ_L in Equation 2) is depicted in Figure 8(b).

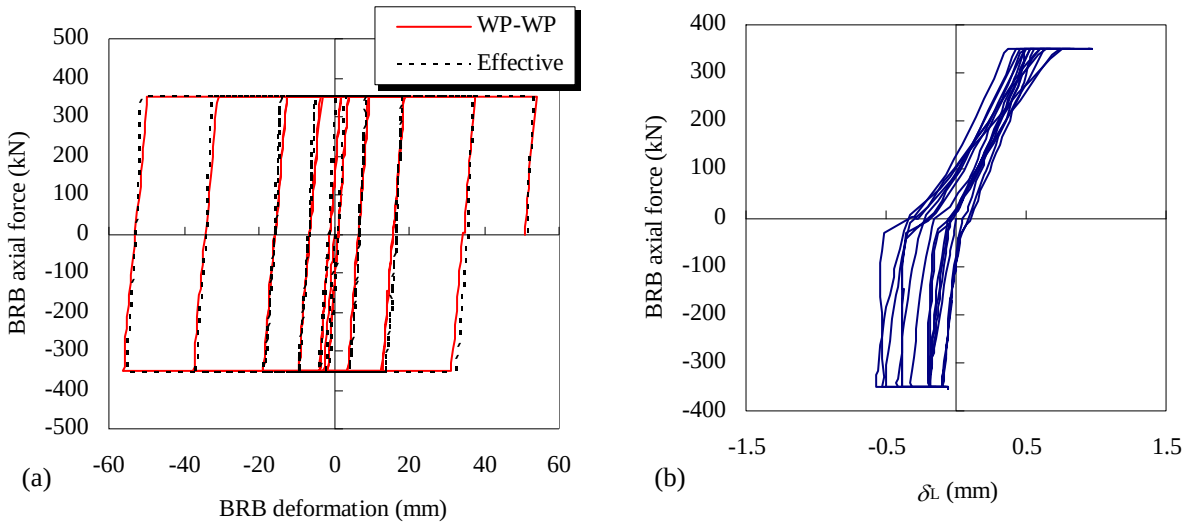

Figure 8. Deformation of the lower BRB in Specimen No.3-Weak corbel: a) BRB global deformation; b) Deformation loss in the connections

The connections of all the 4 specimens exhibit large stiffness in compression and relatively smaller stiffness in tension. It is also obvious that δ_L keeps on changing while the BRB force is hold constant. After the artificial BRB yields (i.e. the 500kN actuators hold constant force), δ_L first

increases and then decreases with further increase of the story drift, in some cases even slips into the opposite side (e.g. from elongation to contraction or vice versa). Often, the change of δ_L while BRB force keeps constant is more significant in the elongation side than in the other side, leaving the curves in Figure 8 leaning towards the contraction side. The reason for these unwarranted changes of displacement is still under investigation.

The effectiveness of BRBs can be greatly affected by the deformation loss since it is favorable to concentrate most of the deformation in the yielding part of a BRB to maximize its energy dissipation. To better interpret the deformation loss δ_L obtained in the experiment, a loss ratio is defined as the ratio of the deformation loss δ_L and the maximum change in the work point-to-work point brace length in the current loading cycle, $\delta_{D,max}$, i.e.,

$$\text{Loss ratio} = \delta_L / \delta_{D,\max} \tag{4}$$

Figure 9 summarizes the maximum loss ratios of each specimen. It shows that the loss ratio decreases rapidly with the increase of story drift ratio. The loss ratio can be as high as above 30% when the structural deformation is small, say 1/500 story drift ratio, while the loss ratio drops to around or below 15% as the story drift ratios increase to 1/200, which generally indicates the onset of minor damages in the building (cracking of the concrete member or some non-structural damages). It further decreases to around or below 5% as the deformation of the specimen further increases.

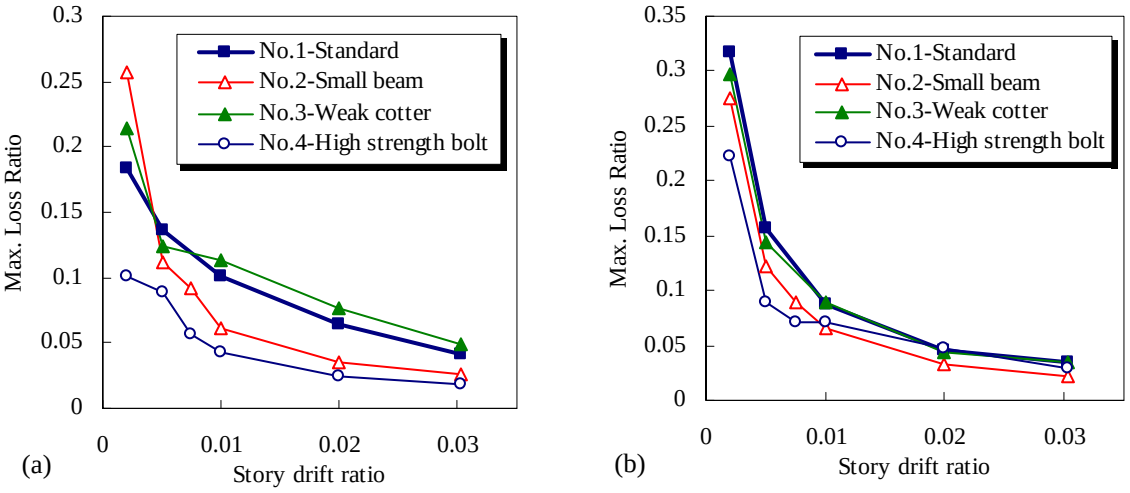

Figure 9. Maximum loss ratios: a) Upper BRB; b) Lower BRB

5 CONCLUSIONS

As an attempt to promote the application of buckling restrained braces in reinforced concrete buildings, the cyclic performance of the connection of the proposed continuously braced frame system is examined through subassembly test. Hybrid controlled loading is employed in the test, in which, instead of using real BRBs, force-controlled actuators are used to simulate the forces transmitted to the connections by BRBs. In such a manner, the requirement to the experimental facilities is much reduced and more effort can be focused on the connections, rather than BRBs. Observations of the test are summarized as below.

(1) Even accounting for the deformation loss in the connection, BRBs yield generally before 1/600 story drift ratio, which is significantly smaller than the deformation that can cause substantial damage to the reinforced concrete frame.

(2) The proposed connections for BRBs impose no extra damages to the concrete beams or columns that are significant enough to discourage this kind of application. The observed cracking pat-

terns suggest that the load bearing condition of the beams and the columns are not significantly changed. For all the specimens, the beams cracked in a flexural or shear-flexural way as in conventional RC frames, the beam-column joints are damaged but not severely up to 1/33 story drift ratio, and the damages to the columns are also minor.

(3) The overall deformation loss in the connection, which includes the elastic deformation of the splice connection of BRB, the relative displacement of the gusset plate as well as the shear deformation of the concrete joint, can contribute a considerable portion (up to 30%) to the overall brace deformation when the structural deformation is very small, e.g. smaller than 1/500 story drift ratio. This corresponds to a state where the BRBs are only slightly yielded. This loss ratio decreases rapidly as the structure's story drift ratio increases and the BRB goes deeper into its plastic range. At 1/50 story drift ratio, the loss ratio would not exceed 10%. And for specimens with smaller beam (Specimen No.2) or higher pretension of the anchor bolts (Specimen No.4), it would not exceed 5%.

ACKNOWLEDGEMENT

This work was supported by the Grants-in-Aid for Scientific Research (A) (22246090). The representative is Akira Wada. The recommendations from the engineers of Kumagaigumi Corp. in designing and preparing the test are also highly appreciated.

REFERENCES

Black, C, J.; Makris, N & Aiken, I D. 2004. Component testing, seismic evaluation and characterization of buckling-restrained braces. *Journal of Structural Engineering, ASCE*. 130(6), 880-894.

Hori, T. 1991. Elasto-plastic behavior of steel brace with restraint system for post buckling. Part 1-5. *Transaction of Annual Meeting,AIJ*. 1435-1478.

Ishii, T.; Mukai, T.; Kitamura, H. et al. 2004. Seismic retrofit for existing R/C building using energy dissipative braces. *Proc. 13th World Conference on Earthquake Engineering.* August 1-6, Vancouver, B.C., Canada, Paper No. 1209.

Kamiya, M.; Simokawa, H.; Morino, S. et al. 1997. Elasto-Plastic Behavior of Flat-Bar Brace Stiffened by Square Steel Tube. *Summaries of Technical Papers of Annual Meeting, AIJ*. C-1, 789-792

Ogawa, Y.; Isoda, K.; Kitamura, Y. et al. 2004. Experimental study on the structural properties of high strength reinforced concrete frames with brace dampers. *Summaries of Technical Papers of Annual Meeting, AIJ*, Hokaido, Japan, 1227-1230

Satsukawa, K.; Ido, K.; Tanaka, T. et al. 2005. Experimental study on failure behavior and energy absorption effect of R/C building with brace type damper based on dynamic cyclic loading. *Journal of Structural and Construction Engineering, Transaction of AIJ*, 591. 129-136.

Tsai, H.C.; Hsiao, P.C.; Wang, K.J. et al. 2008. Pseudo-dynamic tests of a full-scale CFT/BRB frame - Part I: Specimen design, experiment and analysis. *Earthquake Engineering and Structural Dynamics*. 37, 1081-1098

Watanabe, A.; Hitomi, Y; Saeki, E; et al. 1988. Properties of brace encased in buckling-restraining concrete and steel tube. *Proc. 9th World Conference on Earthquake Engineering*. IV, Tokyo & Kyoto, Japan, 617-624